ChemPubSoc Europe

DOI: 10.1002/chem.201600525

CHEMISTRY A European Journal Full Paper

Carbone Structures

Proton Affinities of Cationic Carbone Adducts $[AC(PPh_3)_2]^+$ (A = Halogen, Hydrogen, Methyl) and Unusual Electronic Structures of the Cations and Dications $[AC(H)(PPh_3)_2]^{2+}$

Wolfgang Petz,* Istemi Kuzu,* Gernot Frenking,* Diego M. Andrada, Bernhard Neumüller,* Maximilian Fritz, and Jörn E. Münzer[a]

Abstract: This work reports the syntheses and the first crystal structures of the cationic carbone adducts $[FC(PPh_3)_2]^+$ and $[BrC(PPh_3)_2]^+$ and the protonated dication $[FC(H)(PPh_3)_2]^{2+}$, which are derived from the carbone $C(PPh_3)_2$. Quantum chemical calculations and bonding analyses were carried out for the series of cations $[AC(PPh_3)_2]^+$ and dications $[AC(H)(PPh_3)_2]^{2+}$, where A = H, Me, F, Cl, Br, I. The bonding analysis suggests that the cations are best described as phosphane complexes $L\rightarrow(CA)^+\leftarrow L$ ($L = PPh_3$), which are related to the neutral borylene adducts $L\rightarrow(BA)\leftarrow L$ (L = cyclic carbene; A = H, aryl) that were recently isolated. The carbone adducts $[AC(PPh_3)_2]^+$ possess a π electron lone pair at carbon and they can easily be protonated to the dications $[AC(H)(PPh_3)_2]^{2+}$. The calculations of the dications indicate that the molecules are best represented as complexes $L\rightarrow(CHA)^{2+}\leftarrow L$ ($L = PPh_3$) where a carbene dication is stabilized by the ligands. The central carbon atom in the cations and even in the dications carries a negative partial charge, which is larger than the negative charge at fluorine. There is also the peculiar situation in which the carbon–fluorine bonds in $[FC(PPh_3)_2]^+$ and $[FC(H)(PPh_3)_2]^{2+}$ exhibit the expected polarity with the negative end at fluorine, but the carbon atom has a larger negative charge than fluorine. Given the similarity of carbodiphosphorane $C(PPh_3)_2$ and carbodicarbene $C(NHC)_2$, we expect that analogous compounds $[AC(NHC)_2]^+$ and $[AC(H)(NHC)_2]^{2+}$ with similar features as $[AC(PPh_3)_2]^+$ and $[AC(H)(PPh_3)_2]^{2+}$ can be isolated.

Introduction

Carbones are a class of divalent carbon(0) compounds in which a bare carbon atom retains its four valence electrons as lone pairs with two neutral donor molecules L completing the electron octet in compounds of the general formula CL_2.[1] The bonding situation in carbones that possess dative bonds may be sketched with the formula $L\rightarrow C\leftarrow L$.[2] In contrast, carbenes CR_2 have electron-sharing bonds R–C–R where the central carbon atom has only one electron lone pair. It has been experimentally shown that carbones and carbenes exhibit different chemical reactivities, which is attributed to the number of electron lone pairs.[3] The chemistry of carbones and the heavier group-14 homologues EL_2 (E = C–Pb) has recently been described in a review article.[4]

The majority of carbones show a bent conformation with two lone pairs of electrons with σ and π symmetry. The lone-pair π electrons may engage in π-back-donation, the strength of which depends on the π acceptor ability of L. Stronger π acceptance leads to wider bond angles, which explains the trend in the bending angle from $C(PPh_3)_2$ (131.7°) < $C(PPh_3)(CO)$ (145.6°) < $C(CO)_2$ (156.0°).[2a,4]

Carbones are strong bases that may form addition compounds of type I and II by using one or both lone pairs for donation to Lewis acids A (Scheme 1). However, the filled σ and π orbitals are also able to form double bonds to Lewis acids lacking four electrons for electronic saturation; the most striking type III compounds are the isoelectronic ions $[(Ph_3P)_2C{=}BH_2]^+$[3a] and $[(Ph_3P)_2C{=}CH_2]^{2+}$[5] with the Lewis acids BH_2^+ and CH_2^{2+}, respectively. Another characteristic feature of carbones are the very high first proton affinities (PAs) *and* re-

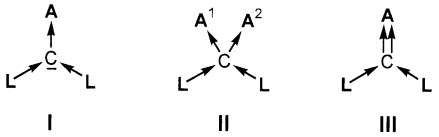

Scheme 1. Schematic description of the bonding situation in adducts of carbones CL_2 with one monodentate Lewis acid A (I), two monodentate Lewis acids A (II), or one bidentate (σ and π) Lewis acid A (III).

[a] *Prof. Dr. W. Petz, Dr. I. Kuzu, Prof. Dr. G. Frenking, Dr. D. M. Andrada, Prof. Dr. B. Neumüller, M. Fritz, J. E. Münzer*
Fachbereich Chemie der Philipps-Universität
Hans-Meerwein-Strasse 4, 35032 Marburg (Germany)
Fax: (+49) 6421/2825653:
E-mail: petz@staff.uni-marburg.de
kuzui@staff.uni-marburg.de
frenking@staff.uni-marburg.de
neumuell@chemie.uni-marburg.de

Supporting information for this article is available on the WWW under http://dx.doi.org/10.1002/chem.201600525.

markably large second PAs, ending up with diprotonated carbones of type II with $A^1, A^2 = H$.[6]

Addition products of carbones are known with transition metals[7] and with main-group Lewis acids.[8] The donor behavior of carbones and carbenes as ligands in transition-metal complexes has been compared in a theoretical study.[9] However, besides diprotonated carbones $[H_2CL_2]^{2+}$, other type II species are restricted to a few examples.

The majority of experimentally known addition compounds belong to type I, where the carbone $C(PPh_3)_2$ serves as the donor species. Hexaphenylcarbodiphosphorane $C(PPh_3)_2$ (**1**) was first synthesized in 1961 by Ramirez, who assumed that **1** has a linear structure.[10] The first X-ray structure of **1** was reported in 1978, which showed that the molecule has a bent equilibrium geometry with a bending angle of 131.7°.[11] Following a theoretical prediction that $C(NHC)_2$ (NHC = N-heterocyclic carbene) should have a similar structure,[12] because NHCs and phosphanes possess comparable ligand properties,[13] the first carbodicarbenes (CDCs) were synthesized showing the typical behavior of carbones.[14] The peculiar bonding properties of CDCs as ligands have recently been utilized by several groups for a range of catalytic reactions such as hydrogenation of inert olefins,[15a] hydroheteroarylation,[15b] intermolecular hydroamination,[15c] and C–C cross-coupling reactions.[15d] The group of Fujii recently reported the extension of the range of carbones to chalcogen-stabilized systems $Ph_2E{\rightarrow}C{\leftarrow}SPh_2(NMe)$ (E = S, Se), which exhibit intriguing reactivities.[16]

Interestingly, tetraaminoallenes (TAAs), which possess a linear structure $(NR_2)_2C{=}C{=}C(NR_2)_2$, can also be viewed as carbones, having similar first and second PAs as carbones.[6] TAAs possess "hidden" or "latent" pairs of electrons that become activated on interaction with main-group or transition-metal Lewis acids, A.[17,18] The π-back-donation $L{\leftarrow}C{\rightarrow}L$ is rather strong when $L = C(NR_2)_2$ but the π acceptor ability of the carbene ligand can be modulated by changing the substituent R. The TAA $(NR_2)_2C{=}C{=}C(NR_2)_2$ with R = methyl has a linear geometry whereas the homologue with R = ethyl has a calculated bending angle of 169.5°.[14b]

Among type I adducts of $C(PPh_3)_2$, the halogen cations $[AC(PPh_3)_2]^+$ (**1 A$^+$**) with A = F (**1 F$^+$**), Cl (**1 Cl$^+$**), Br (**1 Br$^+$**), and I (**1 I$^+$**) are of special interest, because the most electronegative elements F and Cl are formally bonded as cations to a four-electron donor, promising an unusual bonding situation. Furthermore, **1 Cl$^+$** plays a particular key role in the preparation of $C(PPh_3)_2$ and is easily accessible in high yields from PPh_3 and CCl_4.[19] The related cation $[FC(PPh_3)_2]^+$ (**1 F$^+$**) was mentioned in 1983 to be obtained according to Equation (1)[20] but the chemistry and structure of the salt remain unexplored as yet; see also reports on the type II $[F_2C(PR_3)_2]^{2+}$ (**1 F$_2^{2+}$**) dications.[21]

$$3\,Ph_3P + CFBr_3 \rightarrow [FC(PPh_3)_2]Br + Ph_3PBr_2 \qquad (1)$$

Although all type I compounds possess a lone electron pair with π symmetry at C(1), additional uptake of at least the smallest Lewis acid H^+ to give type II compounds is not common and, to the best of our knowledge, restricted to the species $[AC(PPh_3)_2]^+$ with A = H, F, Cl, and Me.[22] In earlier works, we described the protonation of **1 Cl$^+$** to produce **1 Cl(H)$^{2+}$**[23] and the structure of **1 Cl$^+$**.[24] Type II compounds with main-group Lewis acids, A, which have been structurally characterized by X-ray analysis are limited to adducts of a carbone to two boron,[25] two sulfur,[26] and to two fluorine[21] atoms.

In this contribution, we report the first structural proof of **1 Br$^+$**, **1 F$^+$** and the protonated dication **1 F(H)$^{2+}$**. We also calculate the proton affinities (PAs) of **1 A$^+$** with A = H, F, Cl, Br, I, Me and we analyze the bonding situation in the cations **1 A$^+$** and the protonated dications $[AC(H)(PPh_3)_2]^{2+}$ [**1 A(H)$^{2+}$**] with quantum chemical methods.

Experimental Results

The synthesis of **1 F$^+$** proceeds with high yields in dichloromethane according to the procedure reported by Burton and Cox.[20] The ^{31}P NMR signal of **1 F$^+$** in CH_2Cl_2 appears as doublet at $\delta = 21$ ppm with a coupling constant $^2J_{P,F} = 48$ Hz. During work-up procedures of **1 F$^+$**, a further doublet was detected in the ^{31}P NMR spectrum with minor intensity at $\delta = 23$ ppm and a coupling constant of $^2J_{P,F} = 57$ Hz. The signal becomes the main signal upon treating the CH_2Cl_2 solution with ethereal HCl and is attributed to the protonated species **1 F(H)$^{2+}$**. The dication was mentioned previously by Burton,[27] and characterized by multinuclear NMR spectroscopy. An overview of fluorinated ylides was presented by Burton, too.[28] Consistent with the C-protonation of **1 F$^+$**, the ^{19}F NMR spectrum of **1 F(H)$^{2+}$** shows a signal at $\delta_F = -213$ ppm coupled to phosphorus ($^2J_{P,F} = 57$ Hz) and to a proton ($^2J_{H,F} = 38$ Hz); ^{13}C and ^1H NMR spectra support this assumption. In going from **1 F$^+$** to **1 F(H)$^{2+}$**, the ^{31}P and ^{19}F NMR signals both experience a low field shift, indicating electron release upon protonation. To our surprise, **1 F$^+$** is more readily protonated than **1 Cl$^+$**. Even solvents like CH_2Cl_2, $HCCl_3$, or just moisture generate **1 F(H)$^{2+}$**, which is not the case with the chlorine analog **1 Cl$^+$**, which is resistant to the action of water. **1 F(H)$^{2+}$** also forms quantitatively if **1 F$^+$** is treated with $BF_3{\cdot}OEt_2$ in CH_2Cl_2; proton abstraction from the solvent is assumed. The dication **1 F(H)$^{2+}$** can easily be deprotonated to **1 F$^+$** upon treatment with $NaNH_2$.

Although **1 Br$^+$** was previously described by Ramirez[10] as being obtained upon bromination of $C(PPh_3)_2$, no further information was available. Alternatively, **1 Br$^+$** (as the bromide) was obtained by us from the reaction of $C(PPh_3)_2$ with CBr_4 in 1,2-Br,F-C_6H_4, as indicated by the signal at $\delta_p = 24$ ppm in the ^{31}P NMR spectrum.[29] Crystals that separated from the reaction mixture turned out to be **1 Br$^+$** as shown by X-ray diffraction analysis. Attempts to protonate the cation **1 Br$^+$** failed; reaction with ethereal HCl ends up with the formation of the known dication $[H_2C(PPh_3)_2]^{2+}$.

Consistent with the NMR analyses, the identities of the compounds **1 F$^+$**, **1 Br$^+$**, and **1 F(H)$^{2+}$** were confirmed by single-crystal X-ray diffraction, as illustrated in Figures 1–3. It is interesting to note that structural features of **1 F$^+$**–**1 I$^+$** have parallels in NHC chemistry.[30] This is not surprising, because NHC and phosphanes have similar ligand properties and the struc-

tures of carbodiphosphorane $C(PPh_3)_2$ and carbodicarbene $C(NHC)_2$ are very similar.[12,14]

Molecular structure of $1F^+$

Crystals of $\mathbf{1F}^+$ (as the bromide) were obtained from the reaction between PPh_3 and $CFBr_3$ in the solvent 1,2-Br,F-C_6H_4 on layering the solution with *n*-pentane. The compound crystallizes with two independent molecules in the unit cell, with nearly identical parameters and without including solvent molecules (Figure 1). An exactly planar arrangement is found

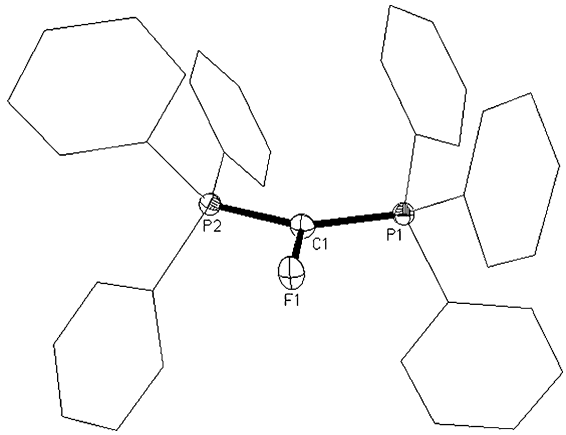

Figure 1. Molecular structure of one of the independent cations of $[FC(PPh_3)_2]Br$ (**1F**Br). The phenyl rings are represented as thin lines; the counter ion Br^- is omitted for clarity. The parameters are given for both independent cations. Selected bond lengths [Å] and angles [°]: C(1)–F(1)/C(38)–F(2) 1.423(3)/1.419(3), C(1)–P(1)/C(38)–P(3) 1.712(3)/1.715(3), C(1)–P(2)/C(38)–P(4) 1.715(3)/1.721(3); F(1)-C(1)-P(1)/F(2)-C(38)-P(3) 111.0(2)/109.2(2), F(1)-C(1)-P(2)/F(2)-C(38)-P(4) 109.6(2)/111.0(2), P(2)-C(1)-P(1)/P(3)-C(38)-P(4) 139.4(2)/139.8(2). Note that the atoms (C1), F(1), P(1), and P(2) of cation 1 correspond to the atoms C(38), F(2), P(3), and P(4) of cation 2.

around the central carbon atom C(1), pointing to a filled p orbital and sp^2 hybridization. A rather long C–F bond length of 1.421 Å (mean value) in $\mathbf{1F}^+$ contrasts with the short one of 1.291 Å in a related NHC-F cation;[31] the latter is in the range of terminally bonded CF ligands in transition-metal complexes.[32] Typical C–F bond lengths, for example, in the anion $(CF_3SO_3)^-$ are found to be about 1.340 Å or in transition-metal complexes with a bridging CF_2 ligand.[33] The lone pair of electrons of π symmetry at C(1) probably experiences some repulsion from the related filled p orbitals at the F atom, whereas in the NHC-F^+ cation some C–F double bond character through back-bonding into a vacant p orbital of the carbon atom is operative. A related elongation is also recorded in going from NHC-Cl^+ (1.686 Å)[34] to $\mathbf{1Cl}^+$ (1.775 Å),[24] from NHC-Br^+ (1.854 Å)[34] to $\mathbf{1Br}^+$ (1.939(2) Å), and from NHC-I^+ (2.042 Å)[35] to $\mathbf{1I}^+$ (2.134 Å).[36] The mean P–C(1) distance of the two independent molecules in $\mathbf{1F}^+$ amounts to 1.716 Å and is slightly shorter than in $\mathbf{1Cl}^+$ (1.722 Å), which may be a hint for increased C–P back-bonding. For the P-C-P angle, an unusually large value of about 140° was recorded, far from the typical angles in other type I addition compounds. Relatively weak bridges exist between phenyl protons and the atoms F or Br. One run produced crystals with strongly disordered F atoms, resulting in a pyramidal arrangement at C(1) ($\mathbf{1F}^+$**-S**); the molecular structure is depicted in the Supporting information (Figure 1 S).

Molecular structure of $1Br^+$

Crystals of $\mathbf{1Br}^+$ (as the bromide) were obtained from 1,2-Br,F-C_6H_4 without including solvent molecules. The molecular structure of the cation $\mathbf{1Br}^+$ is shown in Figure 2. A slight pyramidization of C(1) is found, expressed by the sum of the angles of 358.0°; the carbon atom is located about 0.143 Å out of the Br(1)-P(1)-P(2) plane. A similar embossment was found for the cation of $\mathbf{1I}^+$, whereas the C(1) atoms of $\mathbf{1F}^+$ and $\mathbf{1Cl}^+$ are in an exact planar environment. The P-C-P angles in $\mathbf{1Cl}^+$, $\mathbf{1Br}^+$, and $\mathbf{1I}^+$ are similar (132 ± 1°). No further contacts between the cation and the Br^- anion were found.

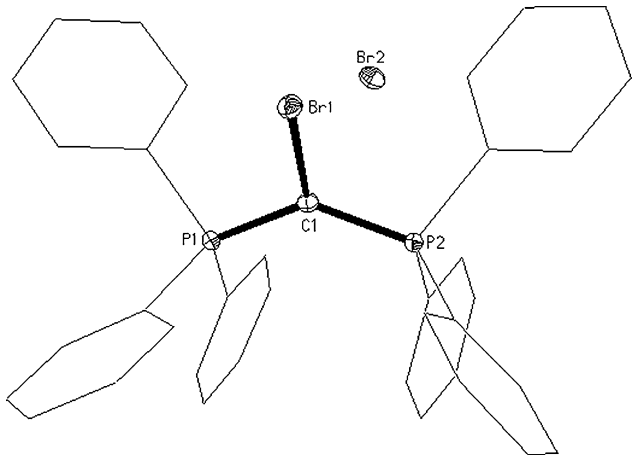

Figure 2. Molecular structure of the cation of $[BrC(PPh_3)_2]Br$ (**1Br**Br). The H atoms at the phenyl rings are omitted for clarity. Selected bond lengths [Å] and angles [°]: C(1)–Br(1) 1.939(2), C(1)–P(1) 1.724(2), C(1)–P(2) 1.726(2); Br(1)-C(1)-P(1) 111.8(1), Br(1)-C(1)-P(2) 112.7(1), P(2)-C(1)-P(1) 133.5(1).

Molecular structure of $1F(H)^{2+}$

Crystals of $\mathbf{1F(H)}^{2+}$ (as the dibromide) were obtained from reacting $\mathbf{1F}^+$ with ethereal HCl in CH_2Cl_2 and the molecular structure of the cation is shown in Figure 3. Crystals separated from a MeCN/toluene solution include a toluene and an additional HCl molecule in the unit cell connected to one of the bromine anions through a Br(1)–H(2)···Cl(1) bridge; the Br(1)–Cl(1) distance amounts to 3.366(2) Å and for the Br(1)–H(2)···Cl(1) angle a value 159.4(5)° was recorded. The other bromine anion forms a contact to the proton at C(1) with a C(1)–Br(2) distance of 3.554(5) Å and a C(1)–H(1)···Br(2) angle of 175°. The C–F bond length does not change markedly upon protonation but the distances of the P atoms to C(1) have experienced the typical elongation to normal single bonds, amounting to a mean value of 1.860 Å usually found in type II compounds. Shrinking of the P-C-P angle to about 121° proceeds upon protonation similarly as in the chlorine analog

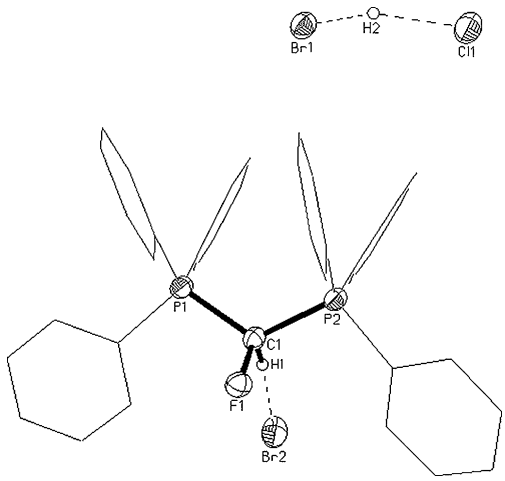

Figure 3. Molecular structure of $(FC(H)(PPh_3)_2)Br_2{\cdot}HCl{\cdot}C_7H_8$ **1 F(H)**$Br_2{\cdot}HCl{\cdot}C_7H_8$). The phenyl rings are represented as thin lines and the solvent molecule is omitted for clarity. Selected bond lengths [Å] and angles [°]: C(1)–F(1) 1.414(6), C(1)–H(1) 1.000, C(1)–P(1) 1.851(5), C(1)–P(2) 1.868(5); F(1)-C(1)-P(1) 108.1(3), F(1)-C(1)-P(2) 105.4(3), P(1)-C(1)-P(2) 120.6(3), F(1)-C(1)-H(1) 107.4, P(1)-C(1)-H(1) 107.4, P(2)-C(1)-H(1) 107.4.

1 Cl(H)$^{2+}$.[23] As a result of another run in CH_2Cl_2 and layering with *n*-pentane, minor quality crystals of **1 F(H)**$Br_2{\cdot}CFBr_3$-S were obtained, however, with nearly identical but less precise parameters (see the Supporting Information).

Quantum Chemical Calculations and Bonding Analysis

From the structures and reactivities of the cationic carbone adducts **1 A$^+$** and the protonated dications **1 A(H)$^{2+}$** emerges the issue of the best description of the bonding situation. The cations **1 A$^+$** can be seen as donor–acceptor complexes between the carbone $C(PPh_3)_2$ and A^+ (Scheme 2, a) or, alternatively, as

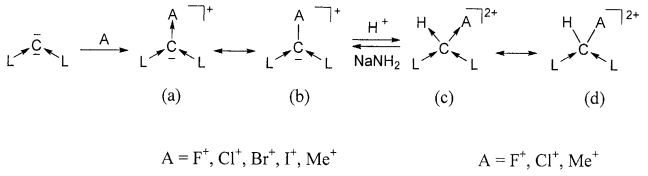

Scheme 2. Schematic descriptions of the bonding situation in adducts of carbones CL_2 with positively charged Lewis acids. The sketches (a) and (b) are alternative views of **1 A$^+$** and the sketches (c) and (d) describe alternative views of the bonding situation in **1 A(H)$^{2+}$**. The bonding analysis suggests that (b) and (d) are preferred.

a complex between the fragment $(CA)^+$ as electron acceptor and two phosphane donor ligands L→$(CA)^+$←L (Scheme 2, b). The latter bonding motif has recently been realized in the related neutral boron compounds L→(BH)←L with L = cAAC (cyclic alkyl aminocarbene)[37] and L→(BA)←L with A = phenyl and L = oxazol-2-ylidene.[38] The same bonding situation is found in the dicarbonyl complex OC→(BTp)←CO where Tp = 2,6-di(2,4,6-triisopropylphenyl).[39] The nature of the chemical bonds in boron compounds L→(BH)←L has previously been studied.[40] To shed light on the bonding situation in **1 A$^+$** and **1 A(H)$^{2+}$**, we carried out quantum chemical calculations and we analyzed the electronic structures.

Figure 4 and Figure 5 show the calculated geometries of the cations **1 A$^+$** and the protonated dications **1 A(H)$^{2+}$** (A = H, Me, F, Cl, Br, I) and the most important bond lengths and angles. Experimental values from previous studies and from this work are given in parentheses. The geometry of the parent system $C(PPh_3)$ (**1**) is shown in Figure 4 for comparison.

The agreement between the theoretical and experimental structures of the mono cations is quite good. The calculated geometries suggest that the C–PPh_3 bonds become significantly longer, from 1.652 Å in the neutral complex **1** to 1.715–1.747 Å in the cations **1 A$^+$**, which agrees with the experimental trend. The C–PPh_3 distances lengthen even more upon further protonation to **1 A(H)$^{2+}$**, where the calculated values are between 1.869–1.920 Å. The X-ray values for the C–PPh_3 bonds are uniformly smaller than the calculated numbers, particularly for the dications (Figure 5). This is likely due to solid-state effects. It has been shown before in a comparison between experimental bond lengths of dative bonds measured in the gas phase and in the solid state that interatomic interactions in the condensed phase are always shorter than in naked molecules.[41] We also investigated the influence of dispersion interactions on the molecular structures, which were found to be unimportant for the present work. Calculations of **1 Me$^+$** and **1 Me(H)$^{2+}$** by using Grimme's D3 term[42] for estimating dispersion forces yielded slightly better agreement between theory and experiment for some geometrical parameters, although others exhibited greater diversion (Figure 3 S, in the Supporting Information).

Theory and experiment agree that the central bond angle P-C-P in **1** (calcd. 136.9°; exp. 131.7°) changes little when one goes to the cations **1 A$^+$** (Figure 4). The calculations suggest that the dications **1 A(H)$^{2+}$** have slightly smaller bond angles for P-C-P (between 125.6°–131.4°) at the tetra-coordinated carbon atom (Figure 5). However, they are still significantly larger than the tetrahedral angle of 109.5°. The experimental P-C-P angles for the dications **1 H(H)$^{2+}$** (123.4°), **1 Me(H)$^{2+}$** (120.1°), **1 F(H)$^{2+}$** (120.6°), and **1 Cl(H)$^{2+}$** (120.8°) are more acute than the calculated values. We think that this comes from the effect of the counter ions, which are found in the vicinity of the H-C-A moiety where they lead to a widening of the latter angle and, thus, to a diminishing of the P-C-P angle.

Table 1 shows the calculated proton affinities (PAs) of the cations **1 A$^+$**. Note that the PA of **1 H$^+$** is the second PA of the parent carbone **1**. The large value of 185.3 kcal mol^{-1} for protonation of the cation, which has been reported before,[6] can be explained by the occurrence of a π electron pair at the central carbon atom, which is left after protonation of one electron lone pair of **1** (Scheme 2 b). Remarkably, the PAs of **1 A$^+$** exhibit little variation with the nature of A. The calculated values have a rather narrow range between 178.7–186.7 kcal mol^{-1}. The PAs of **1 A$^+$** do not depend on the electronegativity of A nor on the presence of lone-pair electrons at A. The calculated value of **1 F$^+$** (186.7 kcal mol^{-1}) is nearly the same as for **1 Me$^+$**

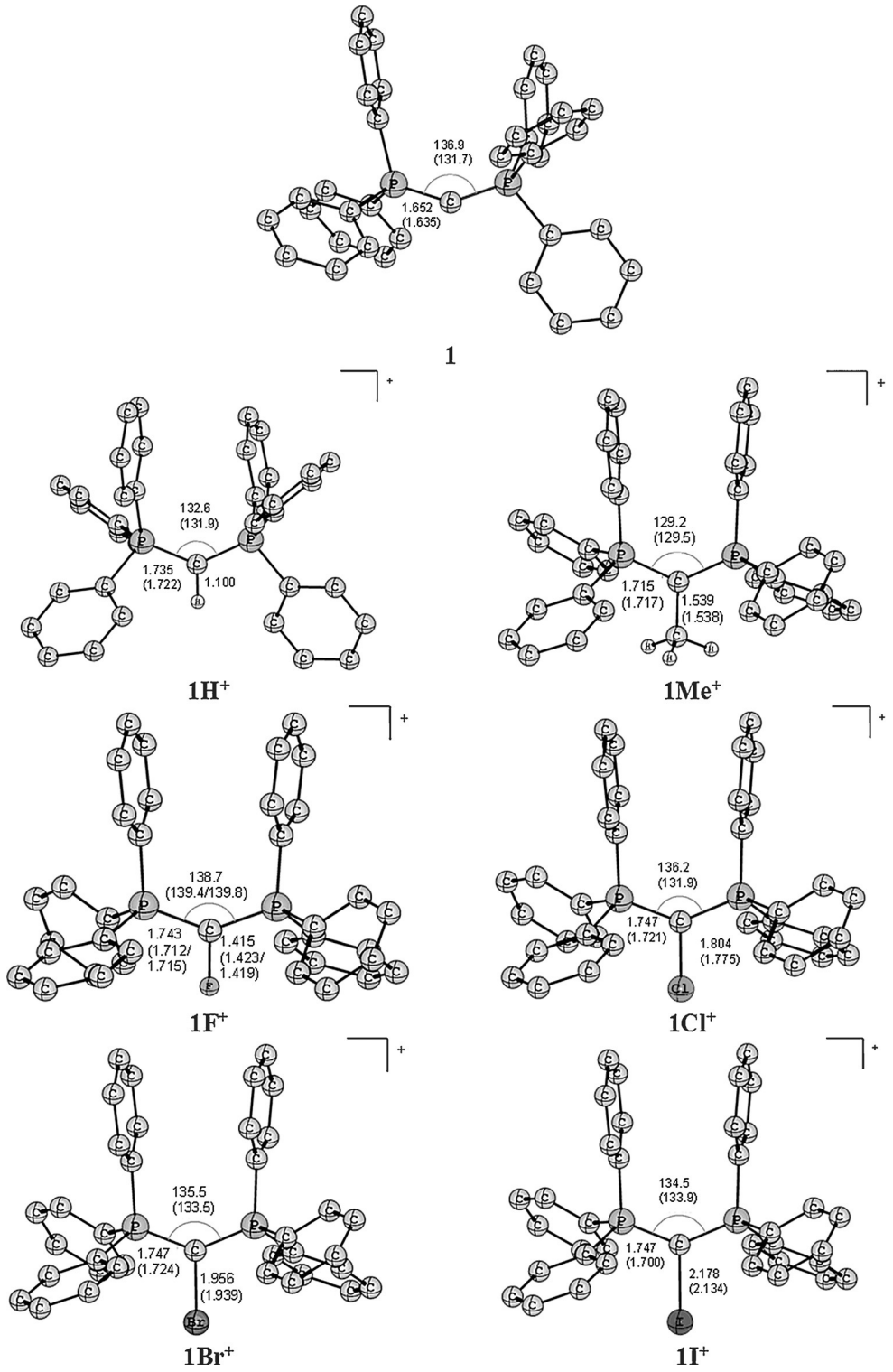

Figure 4. Optimized structures of compounds $\mathbf{1A}^+$ at the BP86/def-SVP&BS level of theory. The numbers in parenthesis are the X-ray data.

(186.6 kcal mol^{-1}). Note that the calculated PA of $\mathbf{1Cl}^+$ (180.1 kcal mol^{-1}) is clearly smaller than that of $\mathbf{1F}^+$, which explains the experimental finding that $\mathbf{1F}^+$ is more readily protonated than $\mathbf{1Cl}^+$.

Table 1 also gives the charge distributions and the polarity of the C–A bonds in the cations $\mathbf{1A}^+$ and the protonated dications $\mathbf{1A(H)}^{2+}$, which provide interesting insight into the electronic structures of the molecules. The central carbon atom in neutral **1** possesses a large negative charge of −1.43 e. The addition of A^+ reduces the negative charge at carbon in the cation $\mathbf{1A}^+$, but it remains rather large, because the $Ph_3P\rightarrow C$ donation becomes stronger in the cation, which

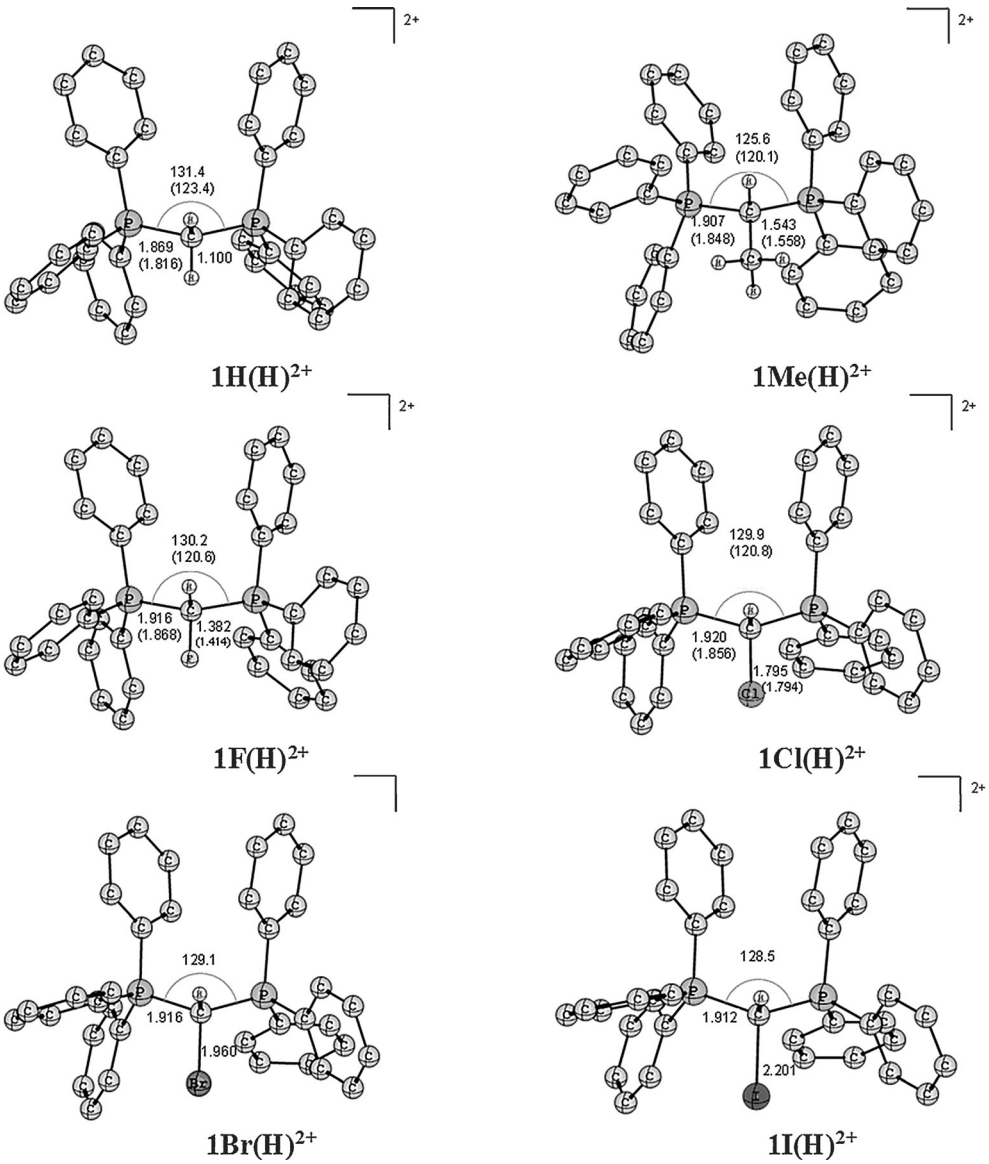

Figure 5. Optimized structures of compounds **1 A(H)$^{2+}$** at the BP86/def-SVP&BS level of theory. The numbers in parenthesis are the X-ray data.

partially compensates for the C→A^{+} charge flow. The partial charges q(PPh$_3$) in **1 A^{+}**, which have rather uniform values between +1.00 and +1.05, are clearly bigger than in **1**. This leads to the curious situation that the central carbon atom in **1 F^{+}** has a higher negative charge (−0.65 e) than fluorine (−0.35 e). Fluorine is more electronegative than carbon, but it can accept a maximum of one electron to reach an electron octet. A negative charge higher than −1.0 e is not possible. Carbon is less electronegative than fluorine, but it can accommodate more than one additional electron. Therefore, it can have a negative partial charge of −1.33 e even in the cation **1 H^{+}** (Table 1).

The results in Table 1 show that the proton affinities of **1 A^{+}** do not correlate at all with the partial charge q(C). The electronic charges at C and A also do not faithfully indicate the polarity of the C–A bond. The natural bond orbitals (NBOs) of the C–A bonds exhibit a polarity that is in agreement with the electronegativities of atom A. That is, the C–F, C–Cl, and C–Br bonds are polarized to the halogen atom whereas the C–I, C–H and C–Me bonds are polarized toward the central carbon atom. The much larger electronic net charge in **1 A^{+}** at carbon comes from the electron lone pair and the charge donation of the phosphane groups Ph$_3$P→C. The latter effect is even stronger than the existence of the lone-pair π electrons. The central carbon atom retains its rather large negative charge even in the dications **1 A(H)$^{2+}$**. Table 1 shows that the calculated values for q(C) are −1.07 in **1 H(H)$^{2+}$** and −1.00 in **1 I(H)$^{2+}$**. Note that the carbon atom in the fluoro dication **1 F(H)$^{2+}$** has a negative partial charge that is slightly larger (−0.35 e) than for fluorine (−0.32 e). Table 1 shows that the polarity of the C–A bonds in the cations **1 A^{+}** changes only little when one goes to the dications **1 A(H)$^{2+}$**.

The very unusual charge distribution in the cations **1 A^{+}** and the dications **1 A(H)$^{2+}$** can be understood by using the bond-

Table 1. Calculated proton affinities (PAs) of the parent carbone **1** and the cations $\mathbf{1A}^+$ in kcal mol^{-1} at the MP2/TZVPP//BP86/SVP level. NBO partial charges in neutral **1** and the cations $\mathbf{1A}^+$ and dications $\mathbf{1A(H)}^{2+}$ at the BP86/TZVPP//BP86/SVP level at the central carbon q(C), substituents q(A), and the phosphane groups $q(PPh_3)$. Polarization of the natural bond orbitals of the C–A bond, Pol(C–A).

Compound	PA	q(C)	$q(PPh_3)$	q(A)	Pol(C–A)
1	+280.0	−1.43	+0.72		
Cations $\mathbf{1A}^+$					
$\mathbf{1H}^+$	+185.3	−1.33	+1.02	+0.30	C (64.8%)–H (35.2%)
$\mathbf{1Me}^+$	+186.6	−1.07	+1.02	+0.04 (−0.64)[a]	C (51.9%)–Me (48.1%)
$\mathbf{1F}^+$	+186.7	−0.65	+1.00	−0.35	C (28.5%)–F (71.5%)
$\mathbf{1Cl}^+$	+180.1	−1.09	+1.05	+0.00	C (45.6%)–Cl (54.4%)
$\mathbf{1Br}^+$	+179.4	−1.17	+1.04	+0.09	C (49.7%)–Br (50.3%)
$\mathbf{1I}^+$	+178.7	−1.26	+1.03	+0.20	C (55.6%)–I (44.4%)
Dications $\mathbf{1A(H)}^{2+}$					
$\mathbf{1H(H)}^{2+}$		−1.07	+1.24	+0.29	C (64.6%)–H (35.4%)
$\mathbf{1Me(H)}^{2+}$		−0.81	+1.22	+0.10 (−0.66)[a]	C (53.2%)-Me (46.8%)
$\mathbf{1F(H)}^{2+}$		−0.35	+1.22	−0.32	C (29.1%)–F (70.8%)
$\mathbf{1Cl(H)}^{2+}$		−0.82	+1.24	+0.06	C (47.5%)–Cl (52.5%)
$\mathbf{1Br(H)}^{2+}$		−0.91	+1.24	+0.15	C (52.1%)–Br (47.9%)
$\mathbf{1I(H)}^{2+}$		−1.00	+1.23	+0.27	C (58.5%)–I (41.5%)

[a] Charge at the methyl carbon atom.

ing models shown in Scheme 2b and d. Support for the assignment of electron-sharing bonds C–A rather than dative bonds C→A in $\mathbf{1A}^+$ and $\mathbf{1A(H)}^{2+}$ comes from EDA[43] (energy decomposition analysis) calculations of the cations and dications by using different fragments for the bonding interactions. The C–A bonds of the cations $\mathbf{1A}^+$ were calculated by using the fragments $\mathbf{1}+A^+$, which come from heterolytic bond breakage of a dative bond, and by using the fragments $\mathbf{1}^+ + A$, which arise from homolytic fission of an electron-sharing bond. Similarly, the EDA calculations of the dications $\mathbf{1A(H)}^{2+}$ were carried out with the fragments $\mathbf{1(H)}^+ + A^+$ (dative bond breaking) and $\mathbf{1H}^{2+} + A$ (fission of an electron-sharing bond). The best description of the bonding model is given by the smallest change in the electronic structure of the fragments upon bond formation, which is indicated by the calculated orbital term ΔE_{orb}.[17a,44] Table 2 and Table 3 show that the EDA calculations for the bond breaking $\mathbf{1A}^+ \rightarrow \mathbf{1}^+ + A$ gives much smaller ΔE_{orb} values than for $\mathbf{1A}^+ \rightarrow \mathbf{1} + A^+$. The results for the dications in Table 4 and Table 5 using the fission model

Table 2. Energy decomposition analysis of $\mathbf{1A}^+ \rightarrow \mathbf{1} + A^+$ (A = H, CH_3, F, Cl, Br, I) at the BP86/TZ2P+//BP86/def-SVP&BS level. Energy values are given in kcal mol^{-1}.

Molecules	$\mathbf{1H}^+$	$\mathbf{1Me}^+$	$\mathbf{1F}^+$	$\mathbf{1Cl}^+$	$\mathbf{1Br}^+$	$\mathbf{1I}^+$
ΔE_{int}	−295.6	−229.6	−474.0	−303.1	−261.4	−216.0
ΔE_{Pauli}	0.0	214.5	348.1	240.7	208.9	169.2
ΔE_{elstat}[a]	−47.8 (16.2%)	−141.9 (31.9%)	−172.9 (21.0%)	−177.0 (32.6%)	−176.5 (37.5%)	−161.5 (41.9%)
ΔE_{orb}[a]	−247.9 (83.8%)	−302.3 (68.1%)	−649.3 (79.0%)	−366.7(67.4%)	−293.7 (62.5%)	−223.6 (58.1%)

[a] The values in parentheses give the percentage contribution to the total attractive interactions $\Delta E_{elstat} + \Delta E_{orb}$.

Table 3. Energy decomposition analysis of $\mathbf{1A}^+ \rightarrow \mathbf{1}^+ + A$ (A = H, CH_3, F, Cl, Br, I) at the BP86/TZ2P+//BP86/def-SVP&BS level. Energy values are given in kcal mol^{-1}.

Molecules	$\mathbf{1H}^+$	$\mathbf{1Me}^+$	$\mathbf{1F}^+$	$\mathbf{1Cl}^+$	$\mathbf{1Br}^+$	$\mathbf{1I}^+$
ΔE_{int}	−117.3	−108.6	−110.2	−85.0	−75.0	−66.3
ΔE_{Pauli}	119.6	242.9	277.3	207.5	182.4	150.3
ΔE_{elstat}[a]	−68.5 (28.9%)	−143.1 (40.7%)	−114.7 (29.6%)	−110.5 (37.8%)	−106.6 (41.4%)	−93.3 (43.1%)
ΔE_{orb}[a]	−168.4 (71.1%)	−208.4 (59.3%)	−272.7 (70.4%)	−182.1 (62.2%)	−150.9 (58.6%)	−123.3 (56.9%)

[a] The values in parentheses give the percentage contribution to the total attractive interactions $\Delta E_{elstat} + \Delta E_{orb}$.

Table 4. Energy decomposition analysis of $\mathbf{1A(H)}^{2+} \rightarrow \mathbf{1(H)}^+ + A^+$ (A = H, CH_3, F, Cl, Br, I) at the BP86/TZ2P+//BP86/def-SVP&BS level. Energy values are given in kcal mol^{-1}.

Molecules	$\mathbf{1H(H)}^{2+}$	$\mathbf{1Me(H)}^{2+}$	$\mathbf{1F(H)}^{2+}$	$\mathbf{1Cl(H)}^{2+}$	$\mathbf{1Br(H)}^{2+}$	$\mathbf{1I(H)}^{2+}$
ΔE_{int}	−210.3	−145.7	−395.0	−218.6	−176.1	−129.8
ΔE_{Pauli}	0.0	217.8	395.4	246.9	206.4	158.6
ΔE_{elstat}[a]	+28.5 (−13.5%)	−75.4 (20.7%)	−114.4 (14.5%)	−111.5 (24.0%)	−107.0 (28.0%)	−86.0 (29.8%)
ΔE_{orb}[a]	−238.8 (113.5%)	−288.0 (79.3%)	−676.0 (85.5%)	−354.0 (76.0%)	−275.4 (72.0%)	−202.3 (70.2%)

[a] The values in parentheses give the percentage contribution to the total attractive interactions $\Delta E_{elstat} + \Delta E_{orb}$.

Table 5. Energy decomposition analysis of $\mathbf{1A(H)^{2+}} \rightarrow \mathbf{1H^{2+}} + A$ (A = H, CH_3, F, Cl, Br, I) at the BP86/TZ2P + //BP86/def-SVP&BS level. Energy values are given in kcal mol^{-1}.

Molecules	$\mathbf{1H(H)^{2+}}$	$\mathbf{1Me(H)^{2+}}$	$\mathbf{1F(H)^{2+}}$	$\mathbf{1Cl(H)^{2+}}$	$\mathbf{1Br(H)^{2+}}$	$\mathbf{1I(H)^{2+}}$
ΔE_{int}	−111.7	−109.3	−111.1	−81.5	−71.4	−62.2
ΔE_{Pauli}	150.9	271.9	335.7	230.6	196.8	155.8
ΔE_{elstat} [a]	−77.5 (29.5%)	−155.5 (40.8%)	−140.2 (31.4%)	−120.9 (38.72%)	−112.2 (41.8%)	−92.4 (42.4%)
ΔE_{orb} [a]	−185.1 (70.5%)	−225.7 (59.2%)	−306.5 (68.6%)	−191.3 (61.28%)	−156.0 (58.17%)	−125.6 (57.6%)

[a] The values in parentheses give the percentage contribution to the total attractive interactions $\Delta E_{elstat} + \Delta E_{orb}$.

$\mathbf{1A(H)^{2+}} \rightarrow \mathbf{1H^{2+}} + A$ also gives smaller ΔE_{orb} values than for $\mathbf{1A(H)^{2+}} \rightarrow \mathbf{1(H)^{+}} + A^{+}$. This is remarkable, because the latter reaction is a charge-separation process. The results support the description of the bonds between **1** and the ligands A with the bond models shown in Scheme 2b and d.

The different electronic structures of the cations $\mathbf{1A^{+}}$ and the dications $\mathbf{1A(H)^{2+}}$ can be examined and visualized with the help of QTAIM (quantum theory of atoms in molecules) calculations.[45] Figure 6 shows the Laplacian distribution $\nabla^2\rho(r)$ of neutral **1** and the cations $\mathbf{1A^{+}}$ in the P-C(A^{+})-P plane and the perpendicular view. The contour line diagrams of the dications $\mathbf{1A(H)^{2+}}$ are shown in Figure 7. The positions of the zero-flux surfaces that are crossing the bond paths nicely indicate the polarity of the bonds. It becomes clear that the C–P bonds are highly polarized toward the carbon end and that the polarity increases with the trend $\mathbf{1} < \mathbf{1A^{+}} < \mathbf{1A(H)^{2+}}$. Note that the shape of the Laplacian distribution for the C–F bond in $\mathbf{1F^{+}}$ clearly shows that the bond is strongly polarized toward fluorine, but there is an area of charge concentration in the π region of carbon, which together with the polarization of the C–P bond yields a large negative partial charge at the carbon atom.

Experimental Section

General

All operations were carried out under an argon atmosphere in dried and degassed solvents by using Schlenk techniques. The solvents were thoroughly dried and freshly distilled prior to use. For the ^{31}P NMR and ^{19}F NMR spectra, we used a Bruker AC 300 spectrometer; ^{13}C and ^{1}H spectra were run on an AC Bruker 300 spectrometer. $[ClC(PPh_3)_2]Cl$ (**1ClCl**) and $[ClC(H)(PPh_3)_2]Cl_2$ (**1Cl(H)**Cl_2) were prepared according to literature procedures.[23] $CFBr_3$ was purchased from Aldrich and stored under an argon atmosphere and dried over molecular sieves. CCDC 1450604 (**1F**Br); 1450605 (1BrBr), 1450606 (**1F(H)**$Br_2{\cdot}HCl{\cdot}C_7H_8$), 1450607 (**1F**Br-S), and 1450608 (**1F(H)**$Br_2{\cdot}CFBr_3$-S) contain the supplementary crystallographic data for this paper. These data are provided free of charge by The Cambridge Crystallographic Data Centre.

Preparation of $(FC(PPh_3)_2)Br$ (1 FBr)

$CFBr_3$ (0.26 mL, 2.7 mmol) was added to a solution of PPh_3 (2.15 g, 8.2 mmol) in 1,4-Br,F-C_6H_4 (ca. 5 mL) and the mixture was stirred at room temperature. After 10 min, the solution turned yellow and after ca. 1.5 h a colorless precipitate formed. The mixture was stirred for 2 days, then, filtered and layered with toluene; the ^{31}P NMR spectrum showed the presence of unreacted PPh_3. On standing for 1 day, crystals of **1F**Br separated. If the reaction was run in CH_2Cl_2, quantitative yield was obtained after 24 h stirring at room temperature. The spectra were run from the CH_2Cl_2 solution. ^{31}P NMR (CH_2Cl_2): $\delta = 20.6$ (d, $^{2}J_{P,F} = 47.8$ Hz) ppm; ^{19}F NMR (CH_2Cl_2): $\delta = -263.0$ (t, $^{2}J_{P,F} = 47.8$ Hz) ppm; ^{13}C NMR ($CDCl_3$): $\delta = 86.6$ (dt, $J_{C,F} = 180.2$ Hz, $J_{C,P} = 135.8$ Hz) ppm. The ^{31}P NMR spectrum of the precipitate showed a singlet at $\delta = 27.2$ ppm. It should be noted that the spectra of the crude material in various solvents were not free from **1F(H)**Br_2. However, solutions of mixtures between **1F**Br and **1F(H)**Br_2 gave solutions of pure **1F**Br when treated with $NaNH_2$.

Preparation of $(FHC(PPh_3)_2)Br_2$ (1 F(H)Br_2)

1FBr (200 mg) was treated with MeCN/toluene in the ratio 10:1 and the ^{31}P NMR spectrum of the solution showed a mixture of **1F**Br and **1F(H)**Br_2 in a 2:1 ratio; addition of a solution of HCl in ether caused the separation of a precipitate, which was dissolved upon addition of CH_2Cl_2. Crystals separated, which turned out to be **1F(H)**$Br_2{\cdot}HCl{\cdot}C_7H_8$. ^{31}P NMR (CH_2Cl_2): $\delta = 23.37$ (d, $^{2}J_{P,F} = 56.84$ Hz) ppm; ^{19}F NMR (CH_2Cl_2): $\delta = -212.8$ (dt, $^{2}J_{P,F} = 56.4$ Hz, $^{2}J_{H,F} = 37.2$ Hz) ppm; ^{13}C NMR ($CDCl_3$): $\delta = 82.6$ (dt, $J_{C,F} = 213.1$ Hz, $J_{C,P} = 49.9$ Hz) ppm; ^{1}H NMR ($CDCl_3$): $\delta = 11.6$ ($^{2}J_{H,F} = 38.0$ Hz, $^{2}J_{H,P} = 6.6$ Hz) ppm.

Formation of $(BrC(PPh_3)_2)Br$ (1 BrBr)

Hexaphenylcarbodiphosphorane (**1**) (150 mg, 0.28 mmol, 2 equiv) was dissolved in about 3 mL 1,2-Br,F-benzene (dried over molecular sieve) in a Schlenk tube. Tetrabromomethane (46.4 mg, 0.14 mmol, 1 equiv) was dissolved in a further Schlenk tube in 3 mL of 1,2-Br,F-benzene. The solutions were combined and the mixture stirred for 10 min at room temperature. The solution turned dark green and a dark precipitate formed. Standing overnight caused the formation of colorless crystals, which turned out to be **1Br**Br. ^{31}P NMR (CH_2Cl_2): $\delta = 24$ ppm.[10,29]

Computational details

Geometry optimizations were performed by using the Gaussian 09 optimizer[46] together with TurboMole6.5[47] energies and gradients at the BP86/def-SVP[48] level of theory. As in the former work,[6] we have used a minimal basis set for the phenyl rings on the PPh_3 groups (benzene BS) except for the α-carbon atoms. The Hessians were computed to determine the nature of the stationary points (one and zero imaginary frequencies for transition states and minima, respectively)[49] and to calculate zero-point energies (ZPEs) as well as thermal corrections and entropy effects by using the standard statistical-mechanics relationships for an ideal gas. To improve the energies, single-point calculations at the MP2/def2-TZVPP[50] were performed on the BP86/def-SVP optimized geometries. For the BP86 and the MP2 calculations, the resolution-of-

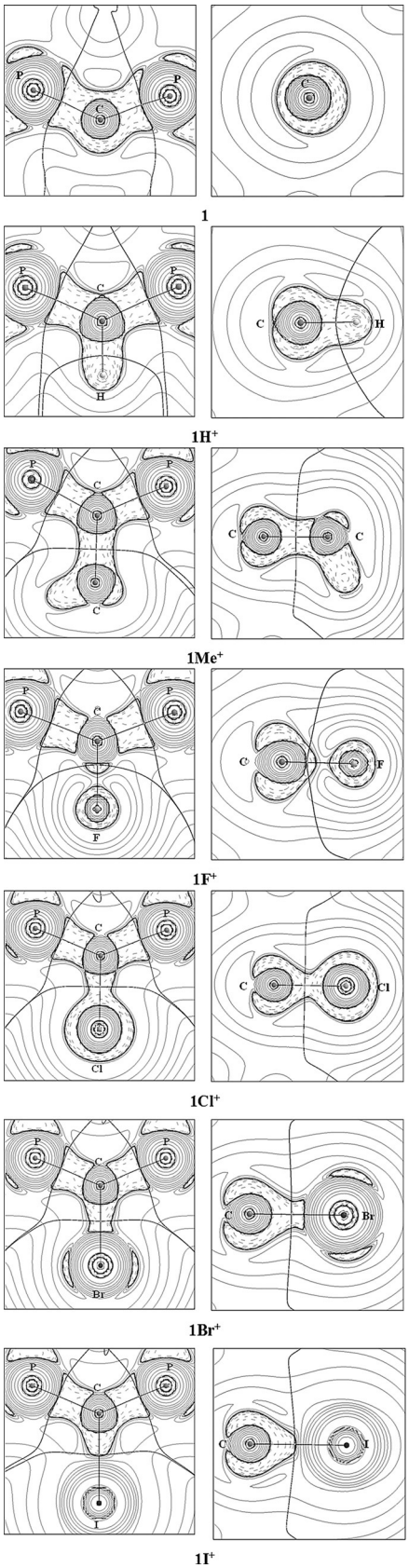

Figure 6. Contour line diagrams of the Laplacian distribution $\nabla^2\rho(r)$ of neutral **1** and the cations **1 A**$^+$ in the parallel (left) and perpendicular (right) P-C-P planes. Dashed lines indicate areas of charge concentration ($\nabla^2\rho(r) < 0$) whereas solid lines show areas of charge depletion ($\nabla^2\rho(r) > 0$). The thick solid lines connecting the atomic nuclei are the bond paths and the solid lines that cross the bond paths show the zero-flux surfaces in the respective plane.

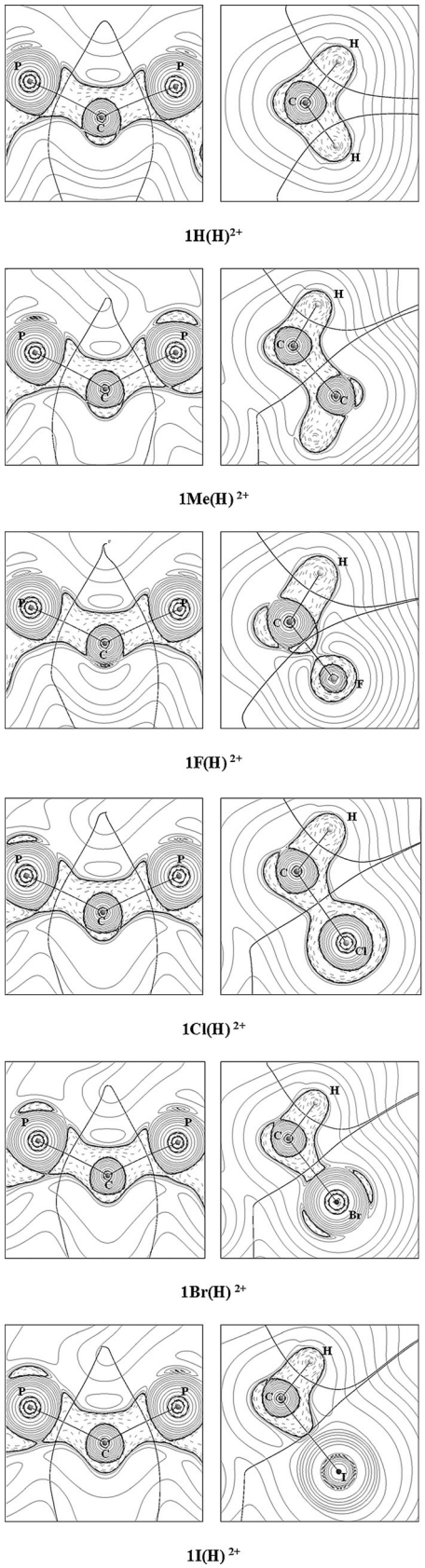

Figure 7. Contour line diagrams of the Laplacian distribution $\nabla^2\rho(r)$ of the dications **1 A(H)**$^{2+}$ in the parallel (left) and perpendicular (right) P-C-P planes. Dashed lines indicate areas of charge concentration ($\nabla^2\rho(r) < 0$) whereas solid lines show areas of charge depletion ($\nabla^2\rho(r) > 0$). The thick solid lines connecting the atomic nuclei are the bond paths and the solid lines that cross the bond paths show the zero-flux surfaces in the respective plane.

identity method has been applied.[51] The NBO partial charges[52] were computed with GENNBO5.9[53] at the BP86/def2-TZVPP level of theory. The analysis of the electron density with the atoms-in-molecules (AIM)[45] method was performed at the BP86/def2-TZVPP level with the AIMAll program package.[54]

The energy decomposition analysis (EDA)[43] was carried with the program package ADF[55] using BP86 in conjunction with uncontracted Slater-type orbitals (STOs) as basis functions (ADF-basis set TZ2P+)[56] at the BP86/def-SVP optimized geometries. The EDA method calculates the instantaneous interaction energy ΔE_{int} between the chosen fragments in the particular electronic reference state and in the frozen geometry of the molecule. This interaction energy is divided into three main components [Eq. (2)].

$$\Delta E_{int} = \Delta E_{elstat} + \Delta E_{Pauli} + \Delta E_{orb} \quad (2)$$

The term ΔE_{elstat} corresponds to the quasiclassical electrostatic interaction between the unperturbed charge distributions of the fragments. The Pauli repulsion ΔE_{Pauli} comprises the destabilizing interactions between electrons of the same spin on either fragment. The orbital interaction ΔE_{orb} accounts for charge transfer and polarization effects. Further details on the EDA method and its application to the analysis of the chemical bond can be found in the literature.[57]

Summary and Conclusion

In this contribution, we present the first crystal structures of the cations **1F$^+$** and **1Br$^+$** where a carbone formally donates a pair of electrons to a halogen cation. The experimental results complement the series of previously known adducts **1A$^+$**, where A = H, Me, Cl, I. The bonding analysis suggests that the compounds are best described as phosphane complexes L→(CA)$^+$←L (L = PPh_3), which are related to the neutral borylene adducts L→(BA)←L (L = cyclic carbene; A = H, aryl) that have recently been isolated. The carbone adducts **1A$^+$** possess a π electron lone pair at carbon and they can easily be protonated to the dications **1A(H)$^{2+}$**. We also present the first structural proof of the fluoro dication **1F(H)$^{2+}$**. Quantum chemical calculations of the dications **1A(H)$^{2+}$** (A = H, Me, F, Cl, Br, I) indicate that the molecules are best represented as complexes L→(CHA)$^{2+}$←L (L = PPh_3) where a carbene dication is stabilized by the ligands. The analysis of the electronic structure shows that the central carbon atom in the cations **1A$^+$** and even in the dications **1A(H)$^{2+}$** carries a negative partial charge that is bigger than the negative charge at fluorine. There is the peculiar situation in which the carbon–fluorine bonds in **1F$^+$** and **1F(H)$^{2+}$** exhibit the expected polarity with the negative end at fluorine, but the carbon atom has a larger negative charge than F. Given the similarity of carbodiphosphorane $C(PPh_3)_2$ (**1**) and carbodicarbene $C(NHC)_2$ (**2**), we expect that analogous compounds **2A$^+$** and **2A(H)$^{2+}$** with similar features as **1A$^+$** and **1A(H)$^{2+}$** can be isolated. The exploration of their reactivity opens the door to new discoveries in the growing field of carbone chemistry.

Acknowledgments

This work was financially supported by the Deutsche Forschungsgemeinschaft.

Keywords: bonding analysis · carbone adducts · proton affinities · quantum chemical calculations

[1] G. Frenking, R. Tonner, *Pure Appl. Chem.* **2009**, *81*, 597.
[2] a) G. Frenking, *Angew. Chem. Int. Ed.* **2014**, *53*, 6040; *Angew. Chem.* **2014**, *126*, 6152. For an opposing viewpoint, see: b) D. Himmel, I. Krossing, A. Schnepf, *Angew. Chem. Int. Ed.* **2014**, *53*, 370; *Angew. Chem.* **2014**, *126*, 378; c) D. Himmel, I. Krossing, A. Schnepf, *Angew. Chem. Int. Ed.* **2014**, *53*, 6047; *Angew. Chem.* **2014**, *126*, 6159.
[3] a) B. Inés, M. Patil, J. Carreras, R. Goddard, W. Thiel, M. Alcarazo, *Angew. Chem. Int. Ed.* **2011**, *50*, 8400; *Angew. Chem.* **2011**, *123*, 8550; b) W.-C. Chen, C.-Y. Li, B.-C. Lin, Y.-C. Hsu, J.-S. Shen, C.-P. Hsu, G. P. A. Yap, T. G. Ong, *J. Am. Chem. Soc.* **2014**, *136*, 914.
[4] G. Frenking, R. Tonner, S. Klein, N. Takagi, T. Shimizu, A. Krapp, K. K. Pandey, P. Parameswaran, *Chem. Soc. Rev.* **2014**, *43*, 5106.
[5] M. A. Celik, W. Petz, B. Neumüller, G. Frenking, *ChemPlusChem* **2013**, *78*, 1024.
[6] R. Tonner, G. Heydenrych, G. Frenking, *ChemPhysChem* **2008**, *9*, 1474.
[7] W. Petz, G. Frenking, *Top. Organomet. Chem.* **2010**, *30*, 49.
[8] W. Petz, *Coord. Chem. Rev.* **2015**, *291*, 1.
[9] T. A. N. Nguyen, G. Frenking, *Chem. Eur. J.* **2012**, *18*, 12733.
[10] F. Ramirez, N. B. Desai, B. Hansen, N. McKelvie, *J. Am. Chem. Soc.* **1961**, *83*, 3539.
[11] G. E. Hardy, J. I. Zink, W. C. Kaska, J. C. Baldwin, *J. Am. Chem. Soc.* **1978**, *100*, 8001.
[12] R. Tonner, G. Frenking, *Angew. Chem. Int. Ed.* **2007**, *46*, 8695; *Angew. Chem.* **2007**, *119*, 8850.
[13] W. A. Herrmann, C. Köcher, *Angew. Chem. Int. Ed. Engl.* **1997**, *36*, 2162; *Angew. Chem.* **1997**, *109*, 2256.
[14] a) C. A. Dyker, V. Lavallo, B. Donnadieu, G. Bertrand, *Angew. Chem. Int. Ed.* **2008**, *47*, 3206; *Angew. Chem.* **2008**, *120*, 3250; b) A. Fürstner, M. Alcarazo, R. Goddard, C. W. Lehmann, *Angew. Chem. Int. Ed.* **2008**, *47*, 3210; *Angew. Chem.* **2008**, *120*, 3254.
[15] a) C. Pranckevicius, L. Fan, D. W. Stephan, *J. Am. Chem. Soc.* **2015**, *137*, 5582; b) C. C. Roberts, D. M. Matías, M. J. Goldfogel, S. J. Meek, *J. Am. Chem. Soc.* **2015**, *137*, 6488; c) M. J. Goldfogel, C. C. Roberts, S. J. Meek, *J. Am. Chem. Soc.* **2014**, *136*, 6227.
[16] T. Morosaki, T. Suzuki, W.-W. Wang, S. Nagase, T. Fujii, *Angew. Chem. Int. Ed.* **2014**, *53*, 9569; *Angew. Chem.* **2014**, *126*, 9723.
[17] Calculations: a) R. Tonner, G. Frenking, *Chem. Eur. J.* **2008**, *14*, 3260; b) R. Tonner, G. Frenking, *Chem. Eur. J.* **2008**, *14*, 3273; c) G. Frenking, R. Tonner, *WIREs Comput. Mol. Sci.* **2011**, *1*, 869; d) G. Frenking, R. Tonner in *Contemporary Carbene Chemistry*, (Eds.: R. A. Moss, M. P. Doyle), Wiley, New Jersey, **2014**, p. 216.
[18] H. G. Viehe, Z. Janousek, R. Gompper, D. Lach, *Angew. Chem. Int. Ed. Engl.* **1973**, *12*, 566; *Angew. Chem.* **1973**, *85*, 581.
[19] R. Appel, F. Knoll, H. Schöler, H.-D. Wihler, *Angew. Chem. Int. Ed. Engl.* **1976**, *15*, 702; *Angew. Chem.* **1976**, *88*, 769.
[20] a) D. J. Burton, D. G. Cox, *J. Am. Chem. Soc.* **1983**, *105*, 650; b) D. J. Burton, *J. Fluorine Chem.* **1983**, *23*, 339.
[21] K. Lauritsen, H. Vogt, L. Riesel, *Z. Anorg. Allg. Chem.* **1994**, *620*, 1103.
[22] a) M. Alcarazo, S. Gomez, S. Holle, R. Goddard, *Angew. Chem. Int. Ed.* **2010**, *49*, 5788; *Angew. Chem.* **2010**, *122*, 5924; b) W. Petz, B. Neumüller, crystal structure of the O_3SCF_3 salt; unpublished results.
[23] W. Petz, B. Neumüller, *Z. Anorg. Allg. Chem.* **2013**, *639*, 2331.
[24] W. Petz, C. Kutschera, S. Tschan, F. Weller, B. Neumüller, *Z. Anorg. Allg. Chem.* **2003**, *629*, 1235.
[25] W. Petz, F. Öxler, B. Neumüller, R. Tonner, G. Frenking, *Eur. J. Inorg. Chem.* **2009**, 4507.
[26] C. Bianchini, A. Meli, A. Orlandini, L. Sacconi, *Angew. Chem. Int. Ed. Engl.* **1980**, *19*, 405; *Angew. Chem.* **1980**, *92*, 1055.
[27] D. G. Cox, D. J. Burton, *J. Org. Chem.* **1988**, *53*, 366.
[28] D. J. Burton, Z.-Y. Yang, W. Qiu, *Chem. Rev.* **1996**, *96*, 1641.

[29] I. Kuzu, J. E Münzer; unpublished results.
[30] N. Kuhn, A. Al-Sheikh, *Coord. Chem. Rev.* **2005**, *249*, 829.
[31] N. Kuhn, H. Bohnen, J. Fahl, D. Blaeser, R. Boese, *Chem. Ber.* **1996**, *129*, 1579.
[32] H. Huang, R. P. Hughes, A. L. Rheingold, *Dalton Trans.* **2011**, *40*, 47.
[33] W. Petz, F. Weller, C. Mealli, J. Reinhold, *Z. Anorg. Allg. Chem.* **2001**, *627*, 1859.
[34] a) N. Kuhn, A. Abu-Rayyan, K. Eichele, C. Piludu, M. Steimann, *Z. Anorg. Allg. Chem.* **2004**, *630*, 495; b) N. Kuhn, A. Abu-Rayyan, M. Ströbele, *Z. Anorg. Allg. Chem.* **2002**, *628*, 2251.
[35] A. J. Arduengo, M. Tamm, J. C. Calabrese, *J. Am. Chem. Soc.* **1994**, *116*, 3625.
[36] a) H. Schmidbaur, C. Zybill, D. Neugebauer, G. Müller, *Z. Naturforsch. Sect. B* **1985**, *40*, 1293; b) W. Petz, S. Heimann, F. Öxler, B. Neumüller, *Z. Anorg. Allg. Chem.* **2007**, *633*, 365.
[37] R. Kinjo, B. Donnadieu, M. A. Celik, G. Frenking, G. Bertrand, *Science* **2011**, *333*, 610.
[38] L. Kong, Y. Li, R. Ganguly, D. Vidovic, R. Kinjo, *Angew. Chem. Int. Ed.* **2014**, *53*, 9280; *Angew. Chem.* **2014**, *126*, 9434.
[39] H. Braunschweig, R. D. Dewhurst, F. Hupp, M. Nutz, K. Radacki, C. W. Tate, A. Vargas, Y. Ye, *Nature* **2015**, *522*, 327.
[40] M. A. Celik, R. Sure, S. Klein, R. Kinjo, G. Bertrand, G. Frenking, *Chem. Eur. J.* **2012**, *18*, 5676.
[41] V. Jonas, G. Frenking, M. T. Reetz, *J. Am. Chem. Soc.* **1994**, *116*, 8741.
[42] S. Grimme, J. Antony, S. Ehrlich, H. Krieg, *J. Chem. Phys.* **2010**, *132*, 154104.
[43] T. Ziegler, A. Rauk, *Inorg. Chem.* **1979**, *18*, 1755.
[44] a) Q. Zhang, W.-L. Li, C.-Q. Xu, M. Chen, M. Zhou, J. Li, D. M. Andrada, G. Frenking, *Angew. Chem. Int. Ed.* **2015**, *54*, 11078; *Angew. Chem.* **2015**, *127*, 11230; b) D. M. Andrada, G. Frenking, *Angew. Chem. Int. Ed.* **2015**, *54*, 12319; *Angew. Chem.* **2015**, *127*, 12494.
[45] a) R. F. W. Bader, *Atoms in Molecules: A Quantum Theory* **1990**; b) R. F. W. Bader, *Chem. Rev.* **1991**, *91*, 893.
[46] Gaussian 09, Revision C.01, M. J. Frisch, G. W. Trucks, H. B. Schlegel, G. E. Scuseria, M. A. Robb, J. R. Cheeseman, G. Scalmani, V. Barone, B. Mennucci, G. A. Petersson, H. Nakatsuji, M. Caricato, X. Li, H. P. Hratchian, A. F. Izmaylov, J. Bloino, G. Zheng, J. L. Sonnenberg, M. Hada, M. Ehara, K. Toyota, R. Fukuda, J. Hasegawa, M. Ishida, T. Nakajima, Y. Honda, O. Kitao, H. Nakai, T. Vreven, J. A. Montgomery, J., J. E. Peralta, F. Ogliaro, M. Bearpark, J. J. Heyd, E. Brothers, K. N. Kudin, V. N. Staroverov, R. Kobayashi, J. Normand, K. Raghavachari, A. Rendell, J. C. Burant, S. S. Iyengar, J. Tomasi, M. Cossi, N. Rega, J. M. Millam, M. Klene, J. E. Knox, J. B. Cross, V. Bakken, C. Adamo, J. Jaramillo, R. Gomperts, R. E. Stratmann, O. Yazyev, A. J. Austin, R. Cammi, C. Pomelli, J. W. Ochterski, R. L. Martin, K. Morokuma, V. G. Zakrzewski, G. A. Voth, P. Salvador, J. J. Dannenberg, S. Dapprich, A. D. Daniels, O. Farkas, J. B. Foresman, J. V. Ortiz, J. Cioslowski, D. J. Fox, Gaussian, Inc., Wallingford, CT, **2009**.
[47] TURBOMOLE V6.5 2013, a development of the University of Karlsruhe and Forschungszentrum Karlsruhe GmbH, 1989–2007; TURBOMOLE GmbH, since **2007**; available from http://www.turbomole.com.
[48] a) A. D. Becke, *Phys. Rev. A* **1988**, *38*, 3098; b) J. P. Perdew, *Phys. Rev. B* **1986**, *33*, 8822; c) A. Schäfer, H. Horn, R. Ahlrichs, *J. Chem. Phys.* **1992**, *97*, 2571.
[49] J. W. McIver, A. Komornicki, *J. Am. Chem. Soc.* **1972**, *94*, 2625.
[50] a) J. S. Binkley, J. A. Pople, *Int. J. Quantum Chem.* **1975**, *9*, 229; b) C. Møller, M. S. Plesset, *Phys. Rev.* **1934**, *46*, 618; c) F. Weigend, R. Ahlrichs, *Phys. Chem. Chem. Phys.* **2005**, *7*, 3297.
[51] a) K. Eichkorn, O. Treutler, H. Öhm, M. Häser, R. Ahlrichs, *Chem. Phys. Lett.* **1995**, *242*, 652; b) F. Weigend, *Phys. Chem. Chem. Phys.* **2006**, *8*, 1057.
[52] A. E. Reed, R. B. Weinstock, F. Weinhold, *J. Chem. Phys.* **1985**, *83*, 735.
[53] E. D. Glendening, J. K. Badenhoop, A. E. Reed, J. E. Carpenter, J. A. Bohmann, C. M. Morales, F. Weinhold, GENNBO 5.9 ed.; Theoretical Chemistry Institute, University of Wisconsin, Madison, WI, **2009**.
[54] T. A. Keith, T. K. Gristmill, 13.05.06 ed. Overland Park KS, USA (http://aim.tkgristmill.com/), **2013**.
[55] G. Te Velde, F. M. Bickelhaupt, E. J. Baerends, C. Fonseca Guerra, S. J. A. Van Gisbergen, J. G. Snijders, T. Ziegler, *J. Comput. Chem.* **2001**, *22*, 931.
[56] E. Van Lenthe, E. J. Baerends, *J. Comput. Chem.* **2003**, *24*, 1142.
[57] a) G. Frenking, F. M. Bickelhaupt, in *The Chemical Bond 1. Fundamental Aspects of Chemical Bonding*, (Eds.: G. Frenking, S. Shaik), Wiley-VCH, Weinheim, **2014**, p. 121; b) F. M. Bickelhaupt, E. J. Baerends, *Rev. Comput. Chem.* **2000**, *15*, 1; c) G. Frenking, K. Wichmann, N. Fröhlich, C. Loschen, M. Lein, J. Frunzke, V. M. Rayón, *Coord. Chem. Rev.* **2003**, *238–239*, 55.

Received: February 3, 2016
Published online on May 11, 2016